



Increasing Oxygen Transfer within the BIONe Single-Use Bioreactor using a Microsparger

Jake McAndrew, MSc and Greg Kauffman

Distek, Inc. | North Brunswick, NJ

Contact: bione@distekinc.com

Abstract

Determining the appropriate bioreactor system configuration for an individual upstream bioprocess can be a challenging task. The nuanced details which differentiate the variety of mammalian cell culture processes will ultimately mean that certain bioreactor configurators will be preferable for specific upstream applications. To optimize typical cell culture performance attributes, such as cell growth and overall productivity, the selection of bioreactor components should be both strategic and data driven. One specific element of a bioreactor system which should be given meaningful consideration is the sparger type. Selection of an appropriate sparger type for a specific upstream bioprocess can be imperative to ensuring that sufficient oxygen mass transfer will be achieved within the bioreactor system.

In this work, we used two types of BIONe Single-Use Bioreactors (SUBs) to characterize the potential difference in oxygen mass transfer between two commonly used sparger types: drilled-hole spargers and microspargers. Using a Design of Experiment (DOE) approach, we generated models which could accurately predict the volumetric mass transfer coefficient of oxygen ($k_L a$) for both systems. Analyzing these models, the difference in mass transfer between the two bioreactor systems could be characterized. Results demonstrated that the use of a microsparger instead of a drilled-holed sparger could drive a two to four-fold increase in $k_L a$ under normal operational conditions within the BIONe SUB. Further analysis of the models suggested that a potential $k_L a$ increase as high as a 6.6-fold may be possible with strategically defined operational parameters. The results also suggested that the microsparger bioreactor may be more appropriate for fed-batch processes, as significant volumetric shifts were observed to have minimal effects on oxygen mass transfer rates within this system.

Introduction

The mass transfer of molecular oxygen within a bioreactor system is essential to support the growth, productivity, and product quality of mammalian cell cultures.^{1,2} Dissolved oxygen (DO) concentrations must be maintained at strategically defined process parameter setpoints. In stir-tank reactor (STR) systems, these concentrations have traditionally been maintained through the sparging of supplemental air and oxygen gases directly into the bioreactor. The sparging of these gases allows for molecular oxygen to be transferred from the gaseous to aqueous phase, a process defined by the oxygen transfer rate (OTR). A suitable OTR is necessary for replenishing oxygen which has been consumed through cellular metabolism. Upstream bioprocesses should be strategically engineered to ensure OTRs are sufficient to maintain defined DO setpoints within bioreactor systems.

The sparger is the component within the system which allows for the transfer of oxygen and air into the bioreactor medium. The sparger typically consists of a length of pipe or tubing

which directs the flow of filtered gases into the bioreactor system. The bioreactor terminus of the sparger often has multiple openings. These openings facilitate the transfer of gases into the bioreactor.

Molecular oxygen has relatively poor solubility within an aqueous medium.³ As such, aspects of the sparger design are often strategically engineered to ensure that a suitable OTR is produced within a bioreactor system. The geometries of the sparger openings at the medium interface are often intentionally designed based upon the oxygen transfer needs of the process. Drilled-hole spargers and microspargers represent two types of gas transfer solutions with distinctly different geometries at this interface.

Drilled-hole spargers are designed with a series of precision cut, uniform circular holes. Hole diameters for many drilled-holed spargers will often be on the order of millimeters. In contrast, a microsparger consists of pores of various sizes, with diameters on the order of microns.



Due to the differences in design, drilled-hole spargers will produce larger diameter bubbles than microsparger options. When volumetric gas flow total is constant, this increased bubble size results in decreased gas-liquid interfacial surface area. This discrepancy has the potential to result in relatively lower OTRs for drilled-hole sparger bioreactors when compared to microsparger systems.

The OTR within a bioreactor system is functionally the product of the oxygen concentration gradient ($C^* - C_L$) and the volumetric mass transfer coefficient of oxygen ($k_L a$), as shown in **Equation 1**. The oxygen concentration gradient is the difference between the dissolved oxygen saturation percentage (C^*) and the dissolved oxygen process value (C_L). For the $k_L a$ term, the k_L term represents the liquid phase mass transfer coefficient, while the a term represents the gas-liquid interfacial surface area per unit volume.⁴

$$\text{Oxygen Transfer Rate} = (C^* - C_L) \times (k_L a)$$

(Eq. 1)

Using the OTR equation (Eq. 1), it can be recognized that increasing the gas-liquid interfacial surface area (a) increases the oxygen transfer rate within a system. This relationship suggests that the utilizing a microsparger could result in relatively higher OTRs within bioreactor systems. Our team recognized that characterizing the magnitude of this difference could be valuable to upstream development bioprocess engineers and scientists. For this study, we generated preliminary data to better describe this difference between these systems.

A Design of Experiment (DOE) evaluation was performed to characterize the effects of volume-dependent operational parameters on the $k_L a$ within a microsparger equipped BIONe Single-Use Bioreactor (SUB). The model resulting from this characterization work was then compared to a mass transfer model previously generated for the drilled-hole sparger BIONe SUB.⁵ Comparing both models, the effects of sparger type on overall bioreactor OTR could be elegantly described to support future process development applications.

Methods and Materials

A BIONe Single-Use Bioreactor (SUB) manufactured by Distek, Inc was utilized for this study. The specific BIONe SUB evaluated was a 2-L system, model number 2022-1001. This model

features a single pitch-blade impeller with right-handed orientation. Gas transfer into the system is facilitated with the use of a microsparger, an element which includes hundreds of pores with diameters of 20 – 40 microns.

To characterize the mass transfer within the microsparger BIONe SUB, a response surface DOE was performed. The input factors for this evaluation were working volume, agitation speed, and bottom air sparge rate. The static gassing-out method was used to determine the $k_L a$ for each set of conditions, as described in de Ory, Romero, and Cantero, 1999.⁶

The evaluation was performed using a model medium which included common cell culture media components. The composition of the model medium was 1.6 g/L sodium bicarbonate, 7.6 g/L sodium chloride, and 0.1% Pluronic F-68. Concentrations were selected based upon previously described mass transfer characterization methods.⁷

The model medium used in this study was supplemented with 30-ppm Simethicone C emulsion. This supplementation served as an antifoaming agent to prevent filter clogging during the evaluation. The concentration of Simethicone C was chosen based upon work which suggested that 30-ppm was suitable for mammalian cell culture processes.⁸

DOE design space bounds were established for the volume-dependent process inputs based upon operational limitations of the equipment. The agitation range chosen for the design space was 100 rpm to 400 rpm. This range represents approximately 20% to 90% of the operational range of the system. Such a range was determined to be suitable for most cell culture applications.

The design space bounds for working volume were defined based upon empirical observations made during method on-boarding. During preliminary mass transfer evaluations, it was noted that at volumes less than 1400 mL, the turbulent agitational flows resulted in erratic and irregular dissolved oxygen measurements. Additionally, at volumes greater than 1800 mL, it was noted that foam levels reached the headplate. This excessive foaming persisted despite the 30-ppm antifoam supplementation. Due to these observations, the working volume for the evaluation design space was defined as 1400 – 1800 mL.

The design space bounds for the air sparge rate were defined based on the results of a limit of detection evaluation performed on the system. At air sparge rates greater than 80 sccm, both



increased variability and a plateauing of the k_La outputs were observed, as shown in **Figure 1**.

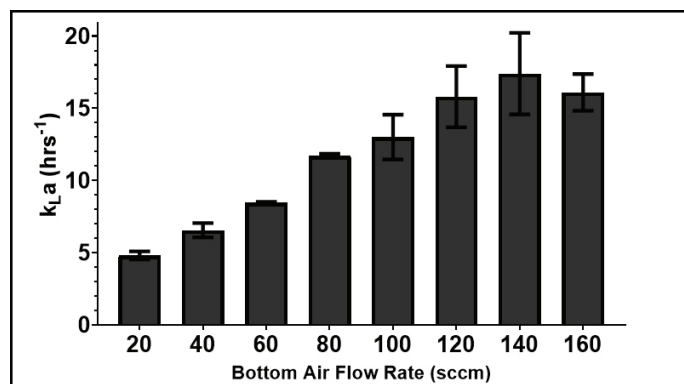


Figure 1: Result from limit of detection evaluation to define upper limit of DOE design space for bottom air sparge rate input factor. Increased variation and output plateauing were observed at sparge at flow rates greater than 80 sccm. Testing conditions were 1400 mL and 400 rpm. Data are mean value from $n = 2$ trials. Bars shown represent standard deviation.

The increased variation observed within the system may have been due to the limitations of the dissolved oxygen probe response time, resulting in increased analytical errors.⁹ Additionally, the plateauing of k_La outputs may have been a consequence of impeller flooding within the system. During such an occurrence, an impeller is surrounded by coalesced gas bubbles and can no longer contact the liquid.¹⁰ This can result in reduced bubble dispersion within the system. Such a reduction in bubble dispersion can decrease the oxygen transfer rate, despite an increased sparged air flow rate. As a result of both the increased variability and plateaued measurements, the DOE design space for the bottom air sparge rate was defined from 20 – 80 sccm. A summary of the overall design space for all three factors is presented in **Table 1**.

Table 1: Design Space for k_La Characterization

DOE Input Factors	Upper Bound of Design Space	Lower Bound of Design Space
Agitation	400 rpm	100 rpm
Working Volume	1800 mL	1400 mL
Bottom Air Sparge Rate	80 sccm	20 sccm

A Box-Behnken response surface design was chosen for the evaluation. This design included 15 sets of different testing conditions. These conditions are presented in **Table 2**.

All conditions analyzed during the characterization were evaluated in duplicate. Upon completion of the k_La determination for all testing conditions, multivariate analysis using a three-factor

ANOVA was performed with the *Fit Model* function of JMP15 (SAS) software.¹¹

Table 2: Experimental Conditions for Box-Behnken Response Surface DOE Evaluation

Pattern	Vessel Volume (mL)	Agitation Rate (rpm)	Sparged Air Flow (sccm)
--0	1400	100	50
0	1600	250	50
-0-	1400	250	20
+0	1800	100	50
0+	1600	100	80
0	1600	250	50
0	1800	400	50
0--	1600	100	20
0++	1600	400	80
0+-	1600	400	20
-0+	1400	250	80
-+0	1400	400	50
0	1600	250	50
+0-	1800	250	20
+0+	1800	250	80
--0	1400	100	50

Results and Discussion

The k_La characterization model generated from the Box-Behnken response surface DOE was evaluated through an actual by predicted linear regression. The regression is shown in **Figure 2**.

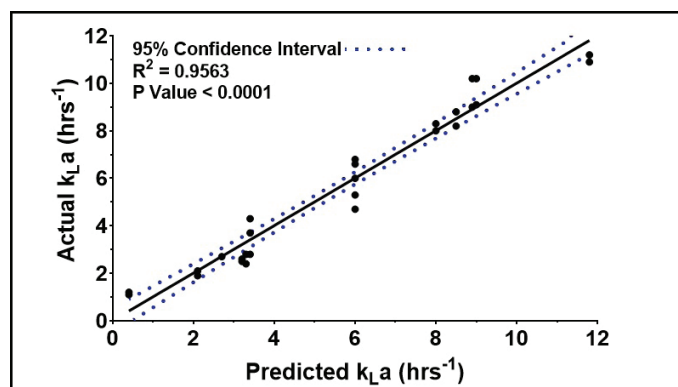


Figure 2: Actual by predicted plot for k_La characterization model of BIOne SUB 2-L microsparger model. The model demonstrates both significance and goodness of fit as indicated by the p-value and correlation coefficient.

These data demonstrate that the microsparger model was highly significant ($p < 0.0001$) and had a strong correlation coefficient ($R^2 = 0.9563$). These characteristics suggest the model appropriately describes the oxygen mass transfer rate within the 2-L microsparger BIOne SUB system.



The accuracy of the model was formally evaluated through a validation assessment. Five sets of B1One SUB operational volume-dependent parameters were randomly generated. All parameters were within the defined design space bounds from the DOE. For each set of operational parameters, the system $k_L a$ was experimentally determined using the static gassing out method. These evaluations were performed in duplicate for each set of testing conditions. For the model to pass the validation assessment, experimentally determined $k_L a$ values had to be within the 95% confidence interval predicted by the model. As shown in **Figure 3**, all conditions met the defined specification for this validation assessment. These data support the predictive accuracy of the model.

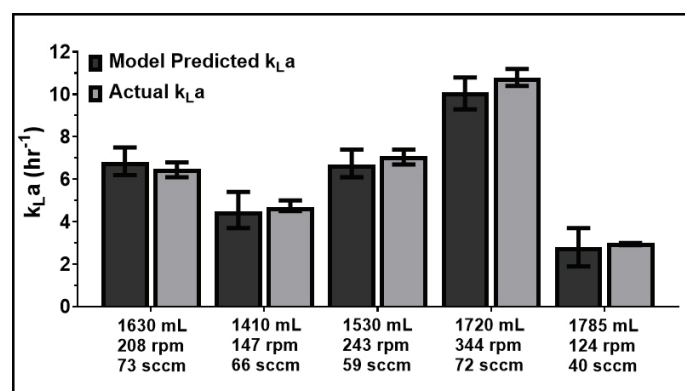


Figure 3: Results from validation evaluation of $k_L a$ characterization model in 2-L microsparger B1One SUB. All sets of testing conditions met defined specification for validation standard. Predicted values include 95% confidence interval, indicated by error bars. Actual values are the mean result from $n = 2$ trials. Bars on actual values represent standard deviation.

To compare the effects of the system inputs on the overall mass transfer within the microsparger and drilled-hole sparger bioreactors, the sum of squares data from the ANOVA analyses were normalized. The individual sum of squares value for each term (i.e. main effect, interaction, or quadratic effect) was normalized to the total sum of squares value for the overall system model (drilled-hole sparger or microsparger system). This normalization strategy is shown in **Equation 2**. The results of this comparison are displayed in the overall *Effects Summary* shown in **Figure 4**.

$$\text{Normalized Effect Percentage} = \frac{\text{Individual Factor Sum of Squares}}{\text{Overall Model Sum of Squares}} \times 100$$

(Eq. 2)

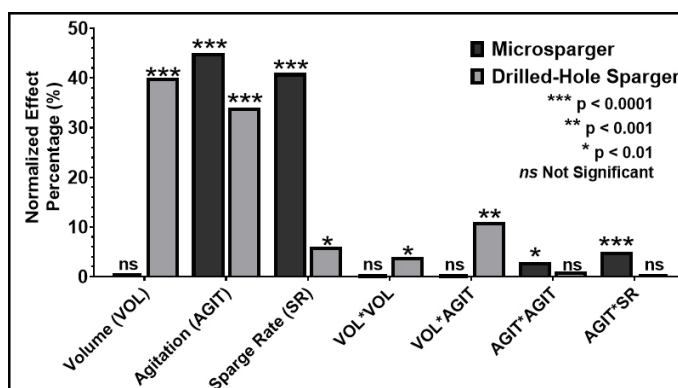


Figure 4: Effect summary comparison of oxygen mass transfer within the 2-L Microsparger and 2-L Drilled-Hole Sparger B1One SUB systems. Comparison demonstrates differences in impact of working volume and sparging rate on overall oxygen mass transfer within both bioreactor systems. P-values represent $\text{Prob} > F$ as calculated by a three-factor ANOVA. Effect interactions and quadratic effects which resulted in normalized effect percentages of less than 1% for both systems were intentionally excluded from figure.

The comparison data shown in **Figure 4** demonstrates that the *Working Volume* and *Sparge Rate* main effect terms had considerably different impacts on the $k_L a$ output between the two bioreactor systems. ANOVA results for the microsparger system suggested that changes in bioreactor working volume would result in no significant changes to overall $k_L a$ of the system. This contrasts with what was previously observed with the drilled-hole sparger system: the normalized effect percentage for the *Working Volume* term was 40% and the ANOVA p-value was < 0.0001 . This attribute may make the microsparger system more appropriate for consistent oxygen transfer within fed-batch processes which involve large volumetric changes.

The normalized effect percentage for the *Sparge Rate* main effect term in the drilled-hole sparger bioreactor was 6%. Within the microsparger bioreactor, this value increased nearly seven-fold to 41%. The respective p-values for the *Sparge Rate* term were 0.0011 and < 0.0001 for the drilled-hole sparger and microsparger systems. This suggests that the sparge rate term within the microsparger bioreactor has a larger impact on overall mass transfer than it does within the drill-hole sparger system.

Both the *Volume*Agitation* interaction term and *Volume*Volume* quadratic term were determined to significantly affect the $k_L a$ output of the drilled-hole sparger bioreactor system. Neither of these terms significantly impacted the $k_L a$ output of the microsparger bioreactor system. Within the microsparger system, *Sparge Rate*Agitation* and *Agitation*Agitation* were the



only interaction and quadratic terms determined to impact the $k_L a$ output. These results align with what was previously observed with the main effect terms.

The results from the effects summary were supported by the three-dimensional response surface plots for both systems, as shown in **Figure 5**. It can be observed that fluctuations in *Sparger Rate* values result in changes to $k_L a$ outputs for both systems. However, these changes are visually more pronounced for the microsparger bioreactor system as compared to the drilled-hole sparger bioreactor system. In contrast, large changes in $k_L a$ outputs can be visually observed with changes to *Working Volume* for the drilled-hole sparger system plots. Such changes in output are not observed in the corresponding the microsparger system plots.

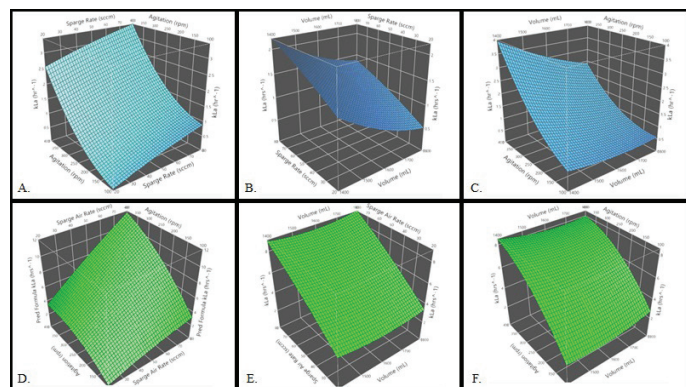


Figure 5: Response Surface plots of oxygen mass transfer within the 2-L Microsparger and 2-L Drilled-Hole Sparger BIOne SUB systems. Drilled-Hole sparger system response surface plots shown in A - C (blue). Microsparger system response surface plots shown in D - F (green). To highlight surface curvature in each model, the z-axes have been normalized to the maximum $k_L a$ output for each individual plot

To gain further application understanding regarding the practical differences of the two sparger types under normal operating conditions, $k_L a$ was modeled at 1400 mL and 250 rpm within both systems ($P/V = 20.3 \text{ W/m}^3$). For this comparison, the bottom air sparge rate was increased stepwise from 20 sccm to 80 sccm in 10 sccm increments (0.014 - 0.057 vvm). The $k_L a$ outputs for both bioreactor systems under these conditions are shown in **Figure 6**. These data visually demonstrate increased rates of oxygen transfer for the microsparger system.

The fold increase for the microsparger system relative to the drilled-hole sparger system was calculated using **Equation 3**. This calculation was performed for each condition. Fold-in-

crease data are summarized in **Figure 7**. A 2-fold to 4-fold increase was observed in $k_L a$ outputs for the microsparger system as aeration was increased across the operational range.

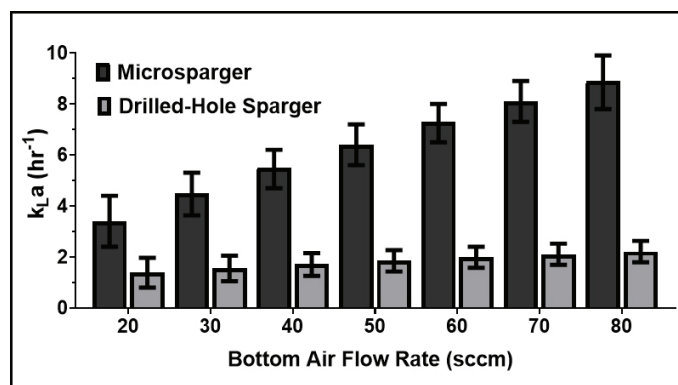


Figure 6: Results from $k_L a$ modeling using 2-L Microsparger and 2-L Drilled-Hole Sparger BIOne SUB systems. Models were evaluated at 1400 mL and 250 rpm ($P/V = 20.3 \text{ W/m}^3$). The $k_L a$ output was calculated as the bottom air sparge rate was increased stepwise from 20 sccm to 80 sccm (0.014 - 0.057 vvm). Data are predicted values with 95% confidence interval.

$$\text{Output Increase for Condition X} = \frac{k_L a \text{ for Condition X (Microsparger System)}}{k_L a \text{ for Condition X (Drilled-Hole Sparger System)}}$$

(Eq. 3)

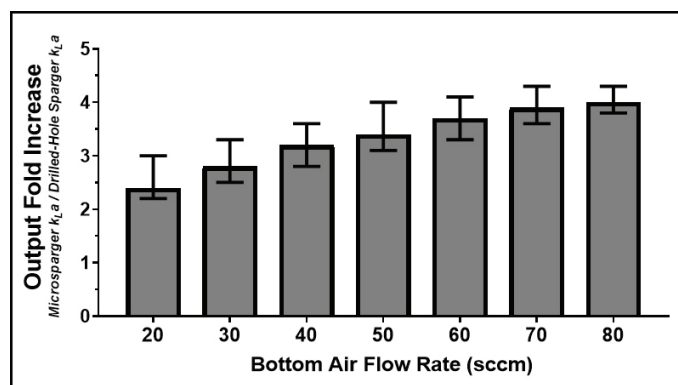


Figure 7: Fold increase in $k_L a$ output between 2-L Microsparger and 2-L Drilled-Hole Sparger BIOne SUB systems under normal operational conditions. Model predicts output increase of approximately 2-fold to 4-fold increase for microsparger system within the design space. The design space was defined as 1400 mL, 250 rpm ($P/V = 20.3 \text{ W/m}^3$), and 20 – 80 sccm (0.014 - 0.057 vvm).



A linear regression was performed for the k_La outputs for each bioreactor model across the defined operational range. The results of this regression are shown in **Figure 8**. The regression slope for the microsparger system was 6.6 times greater than what was calculated for the drilled-hole sparger system ($m = 0.0911$ and $m = 0.0138$, respectively). Assuming minimal impeller flooding, these data suggest that the microsparger SUB OTR may ultimately approach a 6.6-fold increase relative to the OTR within the drilled-hole sparger SUB under normal bioreactor conditions.

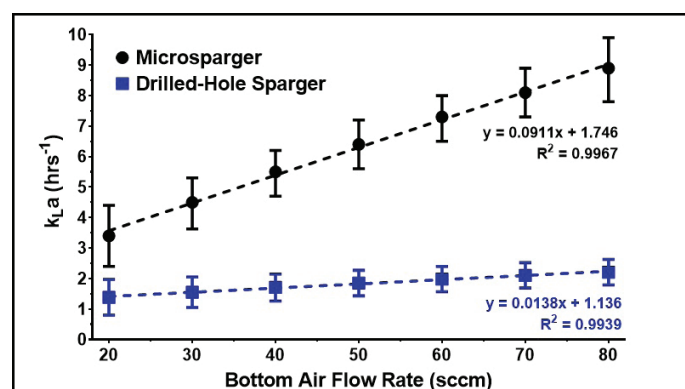


Figure 8: Linear regression from 2-L Microsparger and 2-L Drilled-Hole Sparger BIONe SUB systems. Model simulation results demonstrated that the microsparger can potentially support oxygen transfer at a rate which is 6.6-fold greater than what can be achieved with a drilled-hole sparger system.

Conclusions

Due to the relationship of the gas-liquid interfacial surface area on the bioreactor OTR, it was assumed that the rate of oxygen mass transfer would be increased within the microsparger bioreactor when compared to the rate within a drilled-hole sparger system. To better understand the significance of this increase, we performed a study to characterize k_La within the 2-L microsparger BIONe SUB system. When these results were compared to previous data from a 2-L drilled-hole sparger BIONe SUB, it was demonstrated that an oxygen transfer rate increase of 2-fold to 4-fold is possible when using the microsparger system under normal operating conditions. Maximum increases of up to 6.6-fold may be possible under strategically defined operational parameters.

During the characterization study, it was observed that the microsparger system experienced no significant changes in oxygen mass transfer with changes in bioreactor working volume. This

contrasts what was observed during the previous drilled-hole sparger bioreactor characterization. The drilled-hole sparger bioreactor demonstrated significant fluctuations in system k_La with changes in volume. The oxygen transfer consistency within the microsparger bioreactor may make the system more suitable for use in fed-batch processes, where significant volume changes are common.

While several bioreactor process attributes (i.e. carbon dioxide stripping capacity and hydrodynamic shear forces) should be evaluated when selecting a sparger type, microsparger bioreactor options should be considered to maximize oxygen transfer within a mammalian bioreactor system. As the data from this study demonstrates, a microsparger has the potential to support considerably higher oxygen transfer rates within a bioreactor as compared to drilled-hole sparger options. Thus, the microsparger may be the optimal gas transfer solution for many upstream bioreactor processes.

Acknowledgements

The authors would like to thank Ichor Therapeutics, Inc. for extending laboratory resources to help support the execution of this project. The authors would like to extend specific gratitude to Kyle Parella for his review of this manuscript.



References

1. Yu, L. X., Amidon, G., Khan, M. A., Hoag, S. W., Polli, J., Raju, G. K., & Wood Restelli, V., Wang, M., Huzel, N., Ethier, M., Perreault, H., & Butler, M. (2006). The effect of dissolved oxygen on the production and the glycosylation profile of recombinant human erythropoietin produced from CHO cells. *Biotechnology and Bioengineering*, 94(3), 481-494. doi:10.1002/bit.20875
2. Naciri, M., Kuystermans, D., & Al-Rubeai, M. (2008). Monitoring pH and dissolved oxygen in mammalian cell culture using optical sensors. *Cytotechnology*, 57(3), 245-250. doi:10.1007/s10616-008-9160-1
3. Vendruscolo, F., Rossi, M. J., Schmidell, W., & Ninow, J. L. (2012). Determination of Oxygen Solubility in Liquid Media. *ISRN Chemical Engineering*, 2012, 1-5. doi:10.5402/2012/601458
4. Liu, K., Phillips, J. R., Sun, X., Mohammad, S., Huhnke, R. L., & Atiyeh, H. K. (2019). Investigation and Modeling of Gas-Liquid Mass Transfer in a Sparged and Non-Sparged Continuous Stirred Tank Reactor with Potential Application in Syngas Fermentation. *Fermentation*, 5(3), 75. doi:10.3390/fermentation5030075
5. McAndrew, J. & Kauffman, G. (2020). Upstream Process Development with a $k_L a$ Criterion Within the BiOne Single-Use Bioreactor [White paper]. Distek, Inc. https://www.distekinc.com/wp-content/uploads/2020/10/BiOne-SUB-Upstream-Process-Development-with-a-k_L-a-Criterion_WP.pdf
6. Ory, I. D., Romero, L. E., & Cantero, D. (1999). Laboratory scale equipment for the determination of $k_L a$ in bio-reactors. *Bioprocess Engineering*, 20(1), 73-75. doi:10.1007/pl00009036
7. Matsunaga, N., Kano, K., Maki, Y., & Dobashi, T. (2009). Estimation of dissolved carbon dioxide stripping in a large bioreactor using model medium. *Journal of Bioscience and Bioengineering*, 107(4), 419-424. doi:10.1016/j.jbiosc.2008.11.017
8. Velugula-Yellela, S. R., Williams, A., Trunfia, N., Hsu, C., Chavez, B., Yoon, S., & Agarabi, C. (2018). Impact of media and antifoam selection on monoclonal antibody production and quality using a high throughput micro-bioreactor system. *Biotechnology Process*, 34(1), 262-270. doi:10.1002/btpr.2575
9. Tribe, L. A., Briens, C. L., & Margaritis, A. (1995). Determination of the volumetric mass transfer coefficient ($k_L a$) using the dynamic γ gas out-gas in? method: Analysis of errors caused by dissolved oxygen probes. *Biotechnology and Bioengineering*, 46(4), 388-392. doi:10.1002/bit.260460412
10. Doran, P. M. (2013). *Bioprocess Engineering Principles (Second Edition)*. Academic Press. doi:<https://doi.org/10.1016/C2009-0-22348-8>
11. JMP®, Version <15>. SAS Institute Inc., Cary, NC, 1989-2019.



888.2.DISTEK
 distekinc.com • info@distekinc.com
 121 North Center Drive • North Brunswick, NJ 08902